

Article

Sedimentological Analysis of the Turbidite Sequence in the Northern Part of the West Crocker Formation, Northwest Sabah

Nurul Affah Mohd Radzir ^{*,†,‡}, Che Aziz Ali [‡] and Kamal Roslan Mohamed [‡]

Basin Research Group, National University of Malaysia, Bangi 43600, Selangor, Malaysia

* Correspondence: nurulafifah@ukm.edu.my

† Current address: Geology Program, Department of Earth Science and Environment,

Faculty of Sciences and Technology, National University of Malaysia, Bangi 43600, Selangor, Malaysia.

‡ These authors contributed equally to this work.

Abstract: Gravity-flow deposits form the northern part of the Crocker Formation (Oligocene–Early Miocene), with the most significant interpretation as a sand-rich system in the proximal and a mud-rich system in the distal area of the deep-water turbidite depositional setting. Seven outcrop localities in the northern-part area were selected for mapping and sampling, starting from Kota Kinabalu up to the Telipok area to evaluate the sedimentary sequence. This study used mapping, field observation, and log sketches in the field, as well as extensive analysis and interpretation of sedimentological methods to investigate the sequence of sediment outcrops in the Crocker Formation area of northwest Sabah. During the fieldwork, five main facies were found, namely, massive sandstone facies (f1), graded sandstone facies (f2), laminated sandstone facies (f3), interbedded sandstone and mudstone facies (f4), and mudstone facies (f5). These northern-part outcrops are interpreted as being deposited from the highest to the lowest turbidity currents and the actuality of pelagic mudstone deposition, based on their fining-coarsening-upward pattern. The five geometrical bodies were proposed as laterally contiguous depositional environments, namely, (1) inner fan channel, (2) inner fan channel–levee complex, (3) mid-fan channelized lobes, (4) non-channelized lobes/distal lobes, and (5) basin plains. The facies interpretation shows that the study area consists of lobes, channel–levee complexes, and levees formed in a fan of a deep-water basin setting, with the basinal plain enveloped by thick mudstone deposits. This northern part of the Crocker Formation is interpreted as a multiple-sourced sediment, shelf-fed, Type II, low-efficiency, and sand-rich turbidite depositional system.

Keywords: Crocker Formation; turbidite sequence; deep-water fan system; Sabah



Citation: Mohd Radzir, N.A.;

Ali, C.A.; Mohamed, K.R.

Sedimentological Analysis of the Turbidite Sequence in the Northern Part of the West Crocker Formation, Northwest Sabah. *Appl. Sci.* **2022**, *12*, 12149. <https://doi.org/10.3390/app122312149>

Academic Editors: Gordon Gilja, Manousos Valyrakis, Panagiotis Michalis, Thomas Pahtz and Oral Yagci

Received: 27 October 2022

Accepted: 23 November 2022

Published: 28 November 2022

Publisher's Note: MDPI stays neutral with regard to jurisdictional claims in published maps and institutional affiliations.



Copyright: © 2022 by the authors. Licensee MDPI, Basel, Switzerland. This article is an open access article distributed under the terms and conditions of the Creative Commons Attribution (CC BY) license (<https://creativecommons.org/licenses/by/4.0/>).

1. Introduction

Sediment gravity flow or mass transport process [1] is the movement of sediment that occurs due to the pull of gravity from the top to the bottom of a slope. It is also defined as a sediment flow or sediment fluid mixture influenced by sediment grains moving due to the influence of gravity [2]. The gravity flow and sediment distribution can be affected by the basinal geometries, sediment supply, and also tectonic activity which becomes part of the triggering mechanisms [3,4]. There are two types of gravity-flow sediment which are (i) sediment flow, and (ii) mass transport flow [5–9]. The end product is classified into (i) complex mass transport, (ii) debris flow, (iii) turbidite and debris co-genetics, and (iv) turbidite current.

Turbidite is a dominant sequence of sediments deposited where this process can transport sediments from the shallower to the deep-water basin [10] and can travel further distances and be deposited in large areas if related to a submarine landslide [11]. Turbidite sediments have various characteristics [4], are usually classified based on several dominant components, have different facies characteristics, and can be identified through field observations and also borehole recordings. The three main components are (i) sand and sediment

quantity [12], (ii) flow efficiency [13], and (iii) characteristics of sediment contributors and sediment supply [14], as summarized in Table 1.

Table 1. Summary of characteristics and depositional system [12–14].

Component	Type of System	Characteristics of System
Sand component and quantity of deposits [12]	Type 1: Sand dominant	Formed as a result of sandstone deposition in non-channel or outer lobe areas. Produces sandstone bodies and lobes.
	Type 2: Sand dominant and lack of mud	Formed as a result of the platform or littoral zone contribution. Produces channel–lobes complex and fan–supra lobes.
	Type 3: Mud dominant	Formed from overflows of mud sediment from platforms and slopes. Produces a channel–levee complex.
Flow efficiency [13]	Type 1: Low efficiency	Rich in sand contributed by the shelf. Forming lobes that are dominated by sand sediments.
	Type 2: Medium efficiency	A mixture of sand and silt contributed by fluvial and deltas. Forms aggradation features with mixed lithology.
	Type 3: High efficiency	Rich in fluvial and delta mud. Forming a dominant progradation of mud and sand in the distal area.
Fed-system characteristics and sediment supply [14]	Type 1: Hinterland-fed system	Sediment from toe-slope erosion. Does not have a shelf or a very narrow shelf.
	Type 2: Shelf-fed system	Sediments resulting from river transport, coastal currents, and tidal currents. Dominant with sand. Experience the original transport by waves, tides, and ocean floor currents.
	Type 3: Delta-fed system	Sediment is contributed by rivers. Rich in mud grains.

Understanding gravity-flow sediments is very important in understanding their natural phenomena [15–17] and in the application of science, especially in petroleum exploration and production, determining potential hazards during petroleum production and also determining the risk of geohazards in the future [18]. In northwest Borneo, specifically the Crocker Formation (Figure 1), a large expanse of Paleogene clastic sedimentary rocks of mainly deep-water origin has been outlined by [19–30] and many more. The turbidite succession represents deposition in a tectonically active margin during the subduction of the Proto-South China Sea with the Sunda Shelf opening from Eocene to Holocene [31–33]. In this paper, the sedimentological characteristics of the northern part of the formation are described, based on field observation in the new cutting outcrops of the Pan Borneo Highway, which extends from Kota Kinabalu to the Telipok areas, and includes seven (7) sedimentary rock outcrop localities. The seven localities are as follows: (1) Hap Seng Quarry, Telipok, (2) KFC, UMS, (3) Prime Kondo University, (4) Lorong Suria Inanam, (5) Kg. Divatto, (6) Taman Okk Lojungah, and (7) Pekan Kinarut (Figure 1). Detailed sedimentological work in conjunction with the occurrence of sediment deposits with associated turbidites gives further insight into the sedimentary processes, the depositional setting, and the type of turbidite depositional systems in this Paleogene basin.

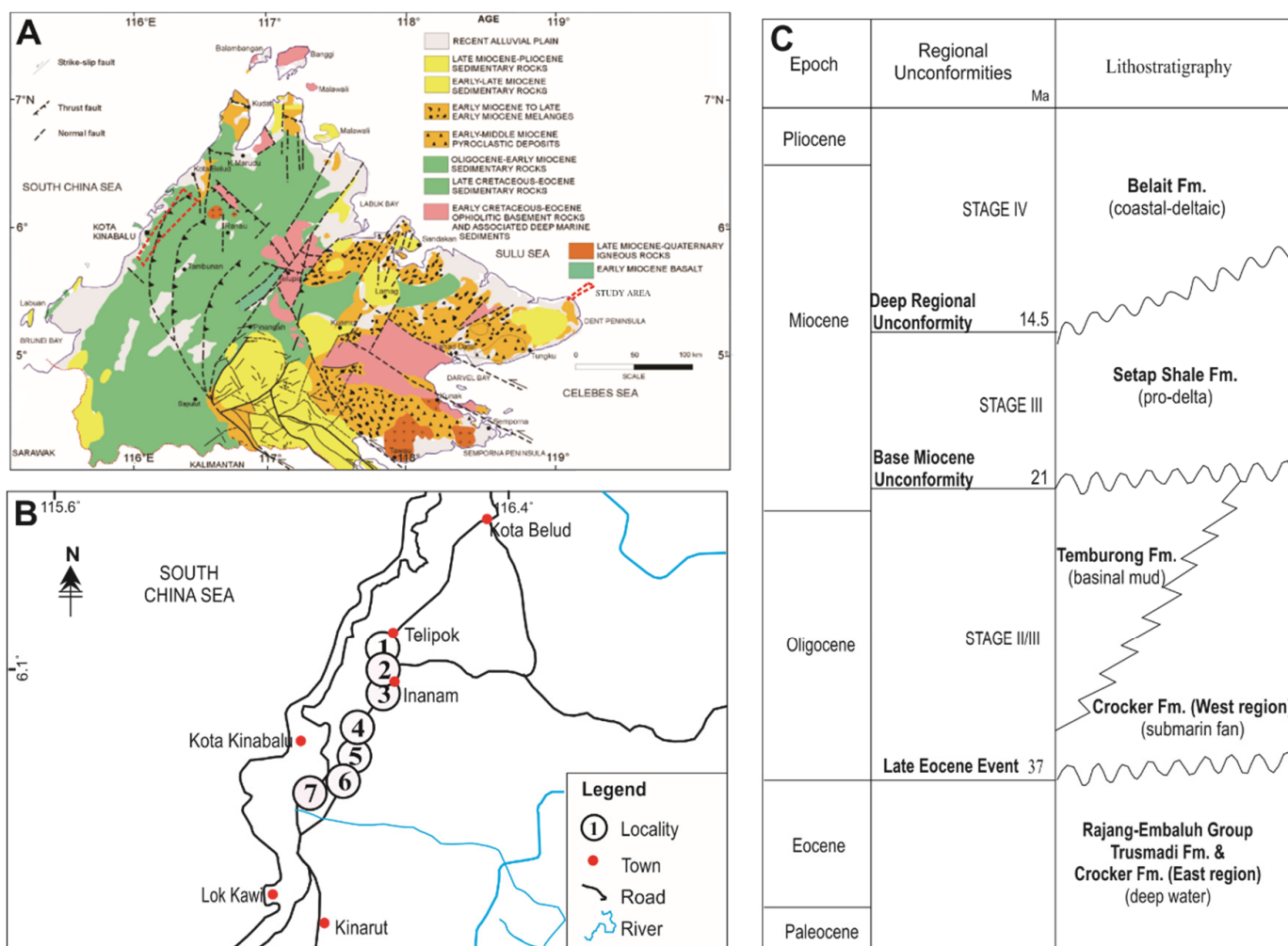


Figure 1. (A) Location of the study area within the geological distribution of Sabah. (B) Location of the outcrops, (1) Hap Seng Quarry, (2) KFC UMS, (3) Prime Kondo University, (4) Lorong Suria Inanam, (5) Kg. Divatto, (6) Taman Okk Lojunjah, and (7) Pekan Kinarut. (C) Chronostratigraphic chart of the Sabah area.

2. Geological Setting

Turbidite and deep-water sedimentary deposits were formed in the Sabah deep-water basin from the late Cretaceous to early Eocene age because of continuous subduction events [34,35]. Late Cretaceous to early Eocene sediments are classified as Trusmadi and the Crocker Formation. This formation consists of sandstone, shale, limestone, and tuff. These sediments were deposited in the central part of the deep-water basin and were then covered by the Rijang-Split Formation of the ophiolite sequence, consisting of ultramafic and mafic rocks [34,36–40]. The sediments were contributed to by drainage from Indo-China [29,41]. During this period, the late Cretaceous Lupar Line, located in the eastern part of Borneo, served as a marker for the shallow-sea platform [42]. The deposited sediments were then deformed and metamorphosed, resulting in phyllites and slates [36,39].

During the Sarawak Orogeny formation event [43], the Rajang Group was thrust and uplifted from the middle Eocene to the late Eocene (Figure 1). During this age, northwest Sabah was dominated by deep-sea marine sediments [29], with the shallow-sea platform advancing northward but still controlled by the Lupar Line. The formation and deposition of sediments in the basin continued to form the Temburong, Setap Shale, and Western Crocker Formations until the Oligocene age. During the early Oligocene age, the shallow-sea platform moved east until it reached the Mersing Line, which is located between the Lupar and the Baram Delta Lines, causing the deposition of delta sediments forming

the Meligan Formation, and limestone shallow marine sediments forming the Melinau Formation around the edge of the Bruneian basin and Sabah [29]. A thick sequence of ocean sediments and deep seabed sediments was deposited in deep troughs in the west and northwest of Sabah. The Crocker Formation is a sequence of deep-sea sediments that have deformed and thrust in this area [34,40,44].

The Crocker Formation in the west consists of sandstone with mudstone/shale, whereas the Crocker Formation in the east (part of the Rajang Group) consists of argillite. The Crocker Formation in the west is younger than the Crocker Formation in the east. During the Sarawak Orogeny (late Eocene), the uplift of the tectonic plates caused and triggered the formation of deep-water sediments, including Crocker, Temburong, and Setap Shale, which are younger than the turbidite deposits of the Rajang Group [28,45] (Figure 1).

3. Materials and Methods

This study involves two stages which are, (i) extensive fieldwork, and (ii) sedimentological work.

3.1. Fieldwork

Extensive fieldwork was performed to get the input of mapping, sedimentological logging, and sampling of the potential exposed outcrops. The data collected included the location of the localities, the determination of the sedimentary structures and fossils, and the measurement of the strike and dip of outcrops. In addition, the thickness of each bed was measured and the changes in the beds were recorded, with photographs being taken to document the outcrops present.

3.2. Sedimentological Work

This stage was performed using facies analysis, facies association analysis, and depositional environment interpretation. This analysis focused on several facies based on the parameters of texture, lithology, sediment structure, and the presence of fossils and trace fossils in the study outcrop sequence. Facies association analysis was performed by classifying the published facies into specific groups and interpreting the depositional environment of the study outcrop sequence.

4. Results

4.1. Facies Analysis

The study area was classified into five main facies, namely, massive sandstone facies (f1), graded sandstone facies (f2), parallel laminated sandstone facies (f3), interbedded sandstone and mudstone facies (f4), and mudstone facies (f5).

4.1.1. Massive Sandstone Facies (f1)

Description: This is a dominant rock layer with coarse to fine sand grains, silt, or mud-sized matrix (<20 percent) and is occasionally found with coarse to very coarse sand grains (<5 percent). These facies are present in single layers and amalgamations with a thickness starting from 10 cm to more than 1 m (Figure 2). The bottom border is sharp and flat, with an eroded and irregular border. Sorting is moderate to good with mud matrix support clasts. The presence of sedimentary structures, such as parallel laminations, fluted casts, load casts, flame structures, tool marks, and rip-up mud clasts was observed. *Cruziana* sp., *Nereites* sp., and *Chondrites* sp. are examples of bioturbation structures (Figures 3 and 4).

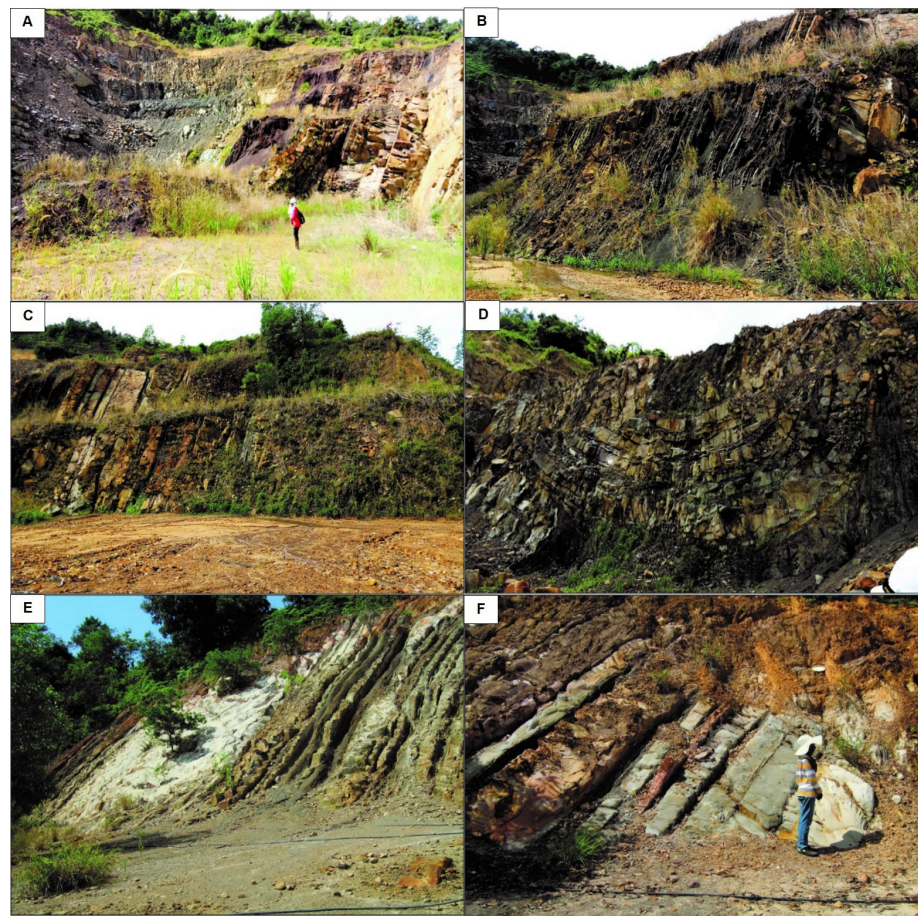


Figure 2. Characteristic examples of lithofacies encountered in the study area. (A) Outcrop section showing the sandstone and mudstone with incline bedded at L1. (B) Outcrop section showing the thickness of the interbedded sandstone and mudstone at L1. (C) Interbedded sandstone and mudstone at L1. (D) Syncline structure in the L1. (E) Outcrops of interbedded sandstone and mudstone in L2. (F) Massive sandstone in L2.

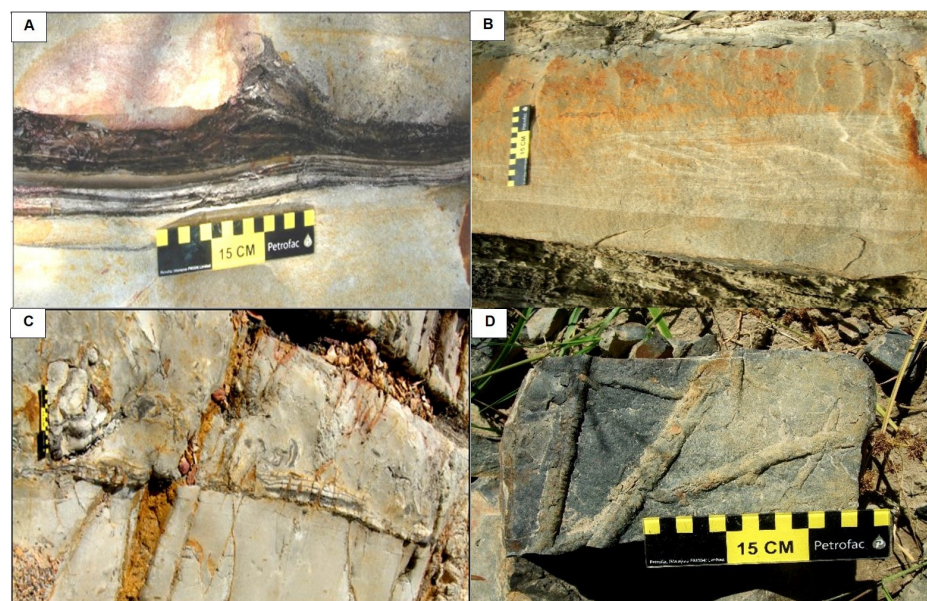


Figure 3. Examples of sedimentary structures in the Crocker Formation. (A) Flame structure found in L1. (B) Complete Bouma sequence from Ta to Tf found in L3. (C) Rip-up mud clasts in L2. (D) *Cruziana* sp. of trace fossils in L2.



Figure 4. Examples of sedimentary structures in the Crocker Formation. (A) Trace fossils were established in the sandstone bed at L1. (B) *Ophiomorpha* sp. originates in the sandstone bed at L3. (C) Water escape structures and convolute structures in the sandstone bed at L3. (D) Flute casts form at the base of a thick sandstone bed at L5. (E) Tool marks trace in the sandstone bed at L7. (F) Coarse sand grain size floated at the base of the graded sandstone bed in L7.

Interpretation: The massive sandstone facies can be formed through two depositional methods, namely, high-density turbidity currents or debris flows [26,43].

4.1.2. Graded Sandstone Facies (f2)

Description: These facies have a fining-upward grain size trend and form a complete to incomplete Bouma sequence (Figures 3–5). The bed at the bottom is sharp, eroded, or irregular, with coarser-sized grains. These facies show poor sorting at the bottom which improves vertically upwards. This facies layer contains parallel, laminated, cross-laminated, and ripple structures.

Interpretation: These facies were deposited because of high to low-concentration turbidite current flow processes, where the movement was not controlled by the matrix concentration [5].

4.1.3. Parallel Laminated Sandstone Facies (f3)

Description: These facies are dominated by fine sand- to silt-sized grains, with a small amount of silt or mud-sized matrix (<20 percent). Parallel lamination is observed in the outcrop sequence layers, but no trace fossils can be found in these facies (Figure 6).

Interpretation: The presence of a powerful current over ripples or dune structures can re-transport fine sand sediment, causing the sediment grains to rearrange in a new layer with a horizontal plane.

4.1.4. Interbedded Sandstone and Mudstone Facies (f4)

Description: The sand-to-mud ratio of these facies is 1:1 or more (>1) according to the layer thicknesses. The sedimentary structures found are wavy and parallel laminations (Figures 6 and 7).

Interpretation: Fine-grained sand sediments were deposited by low-density turbidity currents at the bottom of the water, whereas mud grains are synonymous with suspended transportation in calm energetic currents. Each interbedded deposit formed in conjunction with sand and mudstone showing that sediment deposition occurred at the same time and underwent a transition process [46] or a change in current energy and velocity [47,48].

4.1.5. Mudstone Facies (f5)

Description: These facies contains silt to mud fine sediments. There are parallel lamination-like structures, and no bioturbation traces were found (Figures 6 and 7).

Interpretation: Usually, pelagic or hemipelagic mud sediments are transported through suspension processes [49] before being deposited in open and quiet waters.

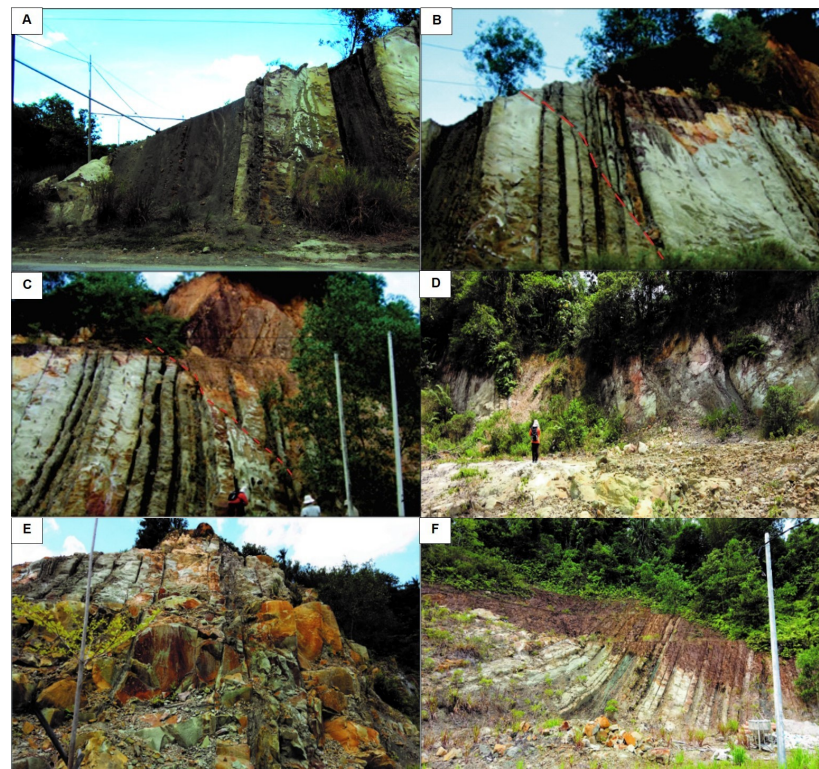


Figure 5. Characteristics of outcrop lithofacies in the study area. (A) Interbedded sandstone and mudstone and also thick sandstone outcrops at the L3. (B) Interbedded sandstone and mudstone, mudstone and massive sandstone with fault structure (red dashed line) at the upper area of L3 outcrop. (C) Sandstone with fault structure (red dashed line) at L3 area. (D) Massive sandstone was found in the L7 area. (E) Interbedded sandstone and mudstone are found in L6. (F) Thick sandstone outcrops show the amalgamation beds in L6.

4.2. Facies Associations

4.2.1. Channels

These facies associations show a fining-upward sequence with sharp (Figures 6 and 7), and well-defined grain size transition sites between each sand-to-mud layer. The upper bed (mudstone facies) occasionally contained mud clasts in the beds (Figure 3). Parallel laminated structures are also found within the sandstone beds. The lower part of these facies associations is dominated by coarse-sized grains (sandstone) transported by high-density turbidity currents. It can also be identified by the presence of current effects such

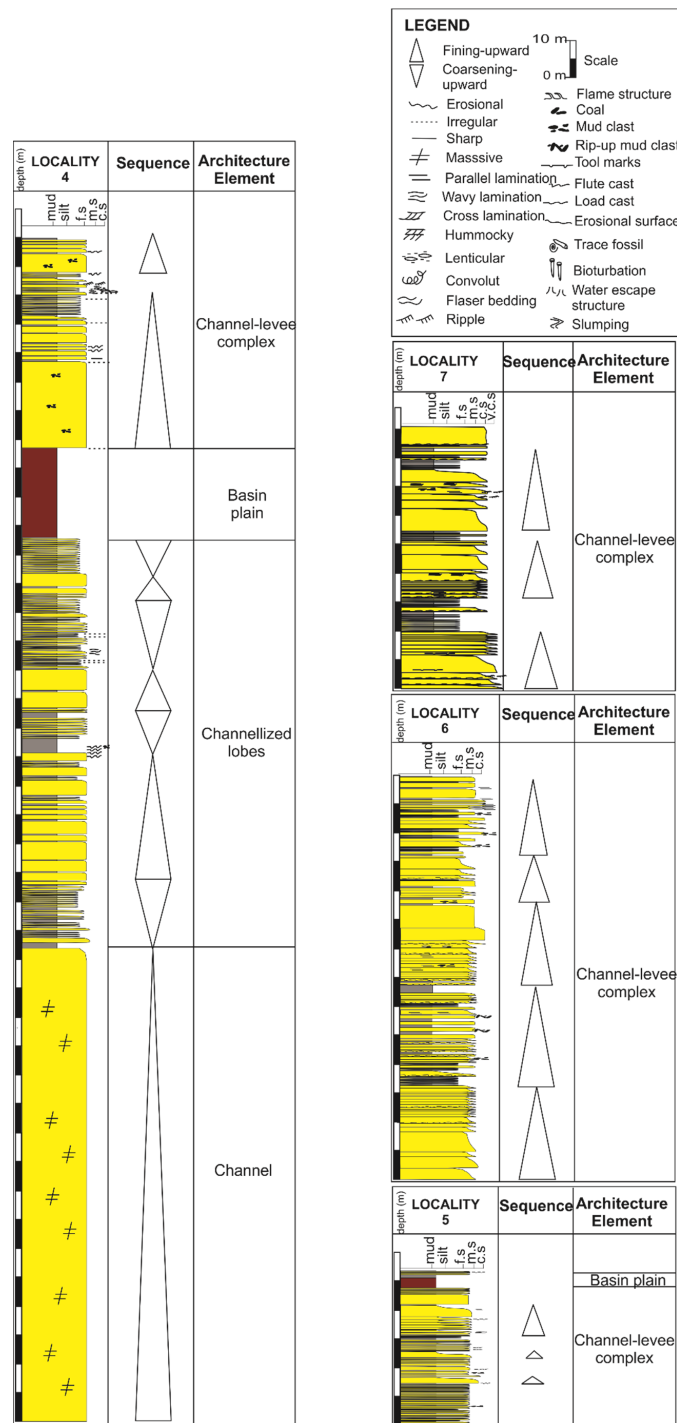


Figure 7. Sedimentary log of L4 to L7, north region of the northwest Crocker Formation.

4.2.3. Lobes

The entire facies association shows an upward thickening and coarsening sequence (Figures 6 and 7). The base structures, such as load casts and flutes are not found at the bottom of the layer, but consist of sand grains with a thin thickness. A vertical sequence that thickens and coarsens upwards indicates that these deposits formed in the lobes.

4.2.4. Basin Plains

These facies associations are pelagic sediments from a very fine sediment fall that are transported in suspension. The deposited pelagic sediments originated from various directions and form a wide and thick spread.

5. Discussion

5.1. Depositional Setting

The study area consists of a deep-water fan system starting from the area of the channels, levees, lobes, and basin plains. All facies associations collect to form a depositional environment based on zones 1, 2, 3, and 4 of the deep-water depositional environment (Figure 8).

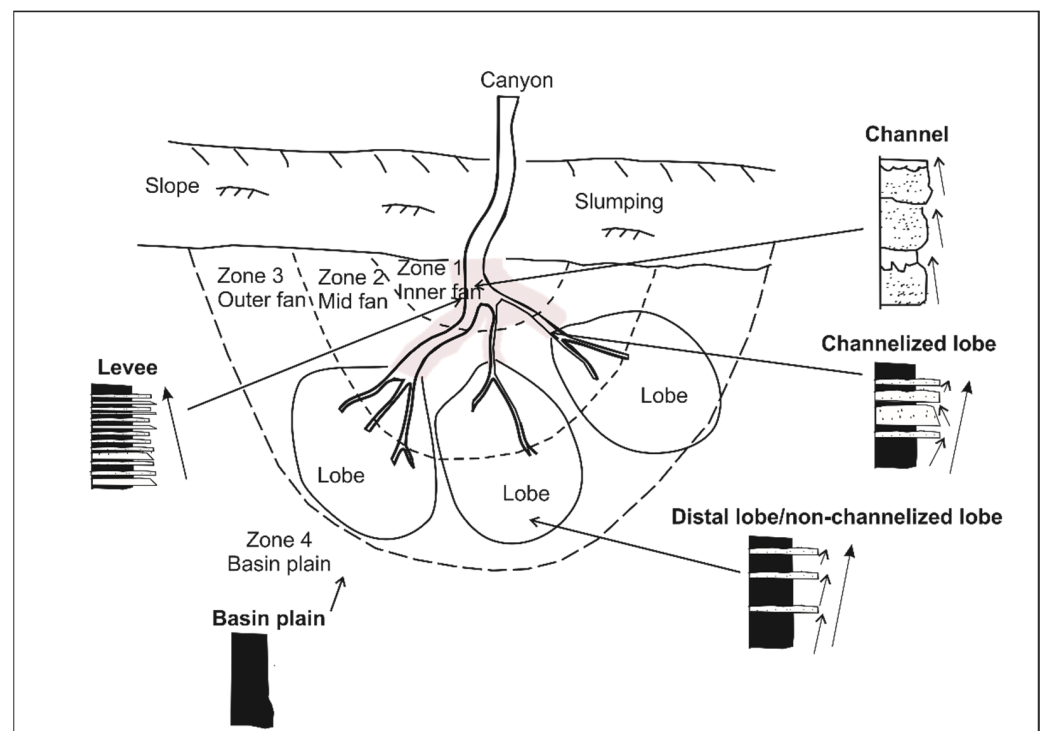


Figure 8. The depositional setting for each component of the facies association interpreted in the study area. Channel shows a fine-upward sequence located in the inner fan (zone 1) part; the levee shows a fine-upward sequence located in the outer channel in the inner and mid fan (zone 1 and zone 2); the channelized lobe shows a coarsening-upward sequence located in the proximal lobe with the presence of a distributary channel, which can be found in the mid fan (zone 2); the distal lobe/non-channelized lobe shows the coarsening-upward sequence located in the distal lobe and no distributary channel are present, which can be found in the outer fan (zone 3); the basin plain is located in the outer of the turbidite fan system.

Zone 1 is the inner fan, consisting of the channel–levees complexes (Figure 8). This proximal area receives its sediments from the canyon and experiences high-density turbidite currents that can transport and deposit sediments ranging in size from coarse sand to medium sand, forming a fining-upward sequence pattern (Figure 8). The proximal area faces a hypoconcentrated density flow where the flow is associated with the matrix strength and grain friction [15]. The density of the flow causes the presence of erosion and records the sharpness and eroded bed (Figure 9). This zone can be a good hydrocarbon accumulation area because it has a high sand content, thick sediment thickness, and good sorting properties with a wider diameter distribution [52].

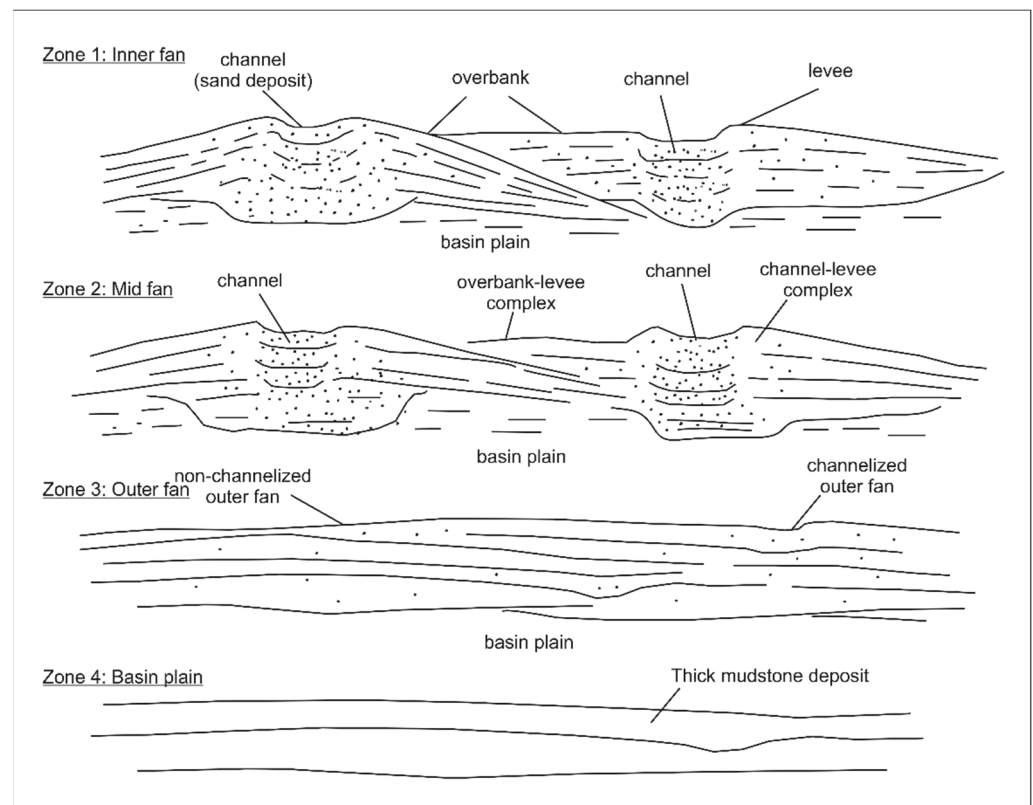


Figure 9. Summary of a depositional model for the northern part of the Crocker Formation. The schematic drawing shows a complete proximal turbidite fan to the basin plain of the deep-water depositional environment in a lateral view.

Zone 2 is the middle fan section consisting of lobes (Figure 8). The lobes in zone 2 consist of channelized lobes and non-channelized lobes. Channelized lobes are distinguished by the presence of channels/distributary channels in the vertical sequence upward of the sedimentary log, as shown in L4 (Figure 7), whereas non-channelized lobes are perceived by the absence of channel sequences in the interpreted vertical sequence. These channelized lobes have a sandstone lithology (f1 and f2) with a medium to thin thickness and a fining-upward sequence pattern and are usually located in the upper lobe (lobe axis) (Figure 8). However, non-channelized lobes are usually located around the proximal lobe to the end lobe, as shown in L1 (Figure 6). These lobes do not show any combination of fining-upward sequence patterns in the entire vertical sequence. This pattern is usually formed by the spreading of the tips of the distributary channels in the upper part of the lobe. However, if there are any edges or slopes in that area, zone 2 is reachable by the tips of distributary channels.

Zone 2 is located in front of zone 1, and their sediment transportation depends on medium to high-density turbidity currents, as well as debris currents (Figure 9). The basis of their sediments support mechanism is equivalent to the concentrated density flows which possess both hypoconcentrated and turbidity current characteristics [15,53]. The medium to high-density turbidite currents was proficient in depositing medium-sized sand sediments with a medium thickness (thickness less than zone 1), good to moderate sorting, and low-matrix content (Figure 10). The transportation of this medium-density turbidity current results in sediment characteristics that have a low-matrix content, high authigenic content, high porosity, and permeability [54]. The entire zone exhibits coarsening-upward sequence characteristics, whereas the presence of distributary channels in the lobes indicates a fine-upward sequence pattern within a vertical coarsening-upward sequence.

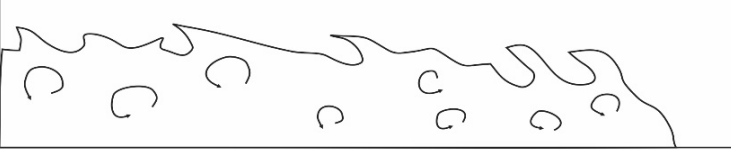
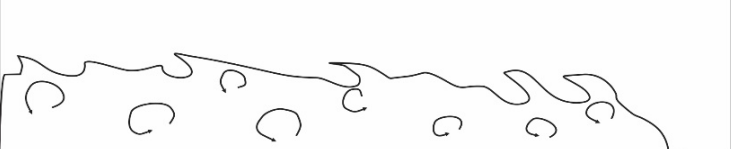
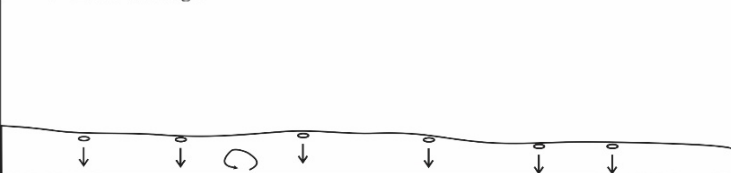
<p>A Zone 1: Higher density turbidity current</p> 	<p>Sediment characteristics</p> <ul style="list-style-type: none"> - Coarse to moderate grain size - Very low matrix content - Very good sorting - Thick bedded sandstone and amalgamated - Present of cast and flute structures - Present of <i>Chondroites sp.</i>, <i>Nereites sp.</i> trace fossils - Hypoconcentrated density flow
<p>B Zone 2: Moderate density turbidity current</p> 	<p>Sediment characteristics</p> <ul style="list-style-type: none"> - Moderate grain size - Low matrix content - Good sorting - Moderate thickness of sandstone bed - Present of cast, flute and tools marks structures - Present of <i>Chondroites sp.</i>, <i>Nereites sp.</i> trace fossils - Concentrated density flow
<p>C Zone 3: Low density turbidity current</p> 	<p>Sediment characteristics</p> <ul style="list-style-type: none"> - Moderate to fine grain size - High matrix content - Moderate sorting - Thin sandstone bed - Thick mudstone bed - Hyperconcentrated density flow
<p>D Zone 4: Pelagic</p> 	<p>Sediment characteristics</p> <ul style="list-style-type: none"> - Fine to very fine grain size - Highest matrix content - Moderate to poor sorting - Very thin sandstone bed to none - Very thick mudstone bed - Prolonged quasi-steady mud-rich flow

Figure 10. Summary of sediment transport behaviors and sediment characteristics of each zone established in this research. (A) Highest turbidity current related to the proximal zone 1 in the inner fan area. (B) Moderate turbidity current related to the mid fan of the zone 2 area. (C) Low turbidity current illustrated by zone 3 in the outer fan area. (D) The pelagic deposited in the basin plain area.

Zone 3 is the area of the distal lobe located in the outer fan of the deep-water depositional environment (Figure 8). This zone is dominated by fine- to very fine-grained layers of thin thickness, with repeated layers, coarsening upwards with the overall sequence. Low-density turbidite currents influence sediment deposition in this zone, which can transport fine-sized sediments to very fine-sized sediments (Figures 9 and 10). Sandstone and mudstone contents are almost equal in the proximal part of the middle lobe, and the mud content is greater than the sandstone in the distal lobe area. The outer lobe is the farthest part of the lobe (distal) and is dominated by fine sediment layers, such as fine sand, silt, and clay [55].

Zone 4 consists of basin plain areas that are characterized by hemipelagic mudstone sediments (with less than a 0.125 or 0.063 mm grain size). Mudstone deposits range in thickness from 2 to 10 m, and coarse grains, such as sand and coarse silt grains, are rarely found (Figure 10). This section is the farthest part of the deep-water fan, and faces a prolonged quasi-steady mud-rich turbidity flow [53,56], forming a broad and widespread expanse of thick mudstone deposits.

5.2. Depositional System

The facies sequence in the fan system in the northern part is dominated by coarse grain sizes such as sandstone with a thick to very thick thickness that forms a channel-levée complex, as well as channel and lobe geometries. The analysis and interpretation of outcrop localities in the northern part of the Crocker Formation show a sand-rich (Type I), low- efficiency (Type I), and shelf-fed (Type II) deep-water turbidite system [12–14] (refer

Table 1). This system is a fan that formed due to the sediment contribution from the shelf, which is rich in the sand but has a small amount of mud sediment. This is in line with the two previous studies which stated that the sediment supply to Crocker Formation is caused by the Sunda Continental Shelf that experienced sediment bypass during the Cenozoic era (middle Eocene to late Oligocene) and Mount Schwaner to the east of Sarawak [57,58]. The supply sediments would have been temporarily deposited in the sediment depocenter on the shelf before being transported again by energy currents such as waves, tides, and turbidite currents, causing numerous sand sediments to be deposited in front of the shelf [59]. With the conjunction of density and turbidity current, the basin provides enough space to accommodate the accumulation and deposition of sediments resulting in the formation of various geometrical bodies such as channels, channels–levee complexes, lobes, and channel–lobes complexes. The distal part of the basinal area is the place of accumulation for the thick mudstone.

6. Conclusions

Based on the sedimentary facies and their evaluation, most of the outcrops in the northern part of the northwest Crocker Formation mostly represent a complete deep-water basin environment. Occasionally, as observed in the outcrops, the intervals of massive sandstone facies (f1), graded sandstone facies (f2), parallel laminated sandstone facies (f3), cross-laminated sandstone facies (f4), interbedded sandstone and mudstone facies (f4) and mudstone facies (f5) form a package of turbidity current influences which are representative of a large-scale turbidite deep-water basin. The turbidite basin, interpreted to consist of geometrical bodies such as channels, levees, lobes, and basin plains, is categorized as a sand-rich, low- efficiency, and shelf-fed system. This system represents the bypass sediment supply during the active subduction of the Proto-South China Sea, with the Sunda Shelf opening from the Eocene to the Holocene age. Such results are in line with previous theories and may be useful as depositional indicators in deep-water depositional settings where the outcrops are sparse, and when integrated with other field data evidence, may provide additional clues to the deposition setting and depositional systems of the Crocker Formation.

Author Contributions: Conceptualization, N.A.M.R.; methodology, N.A.M.R., C.A.A. and K.R.M.; formal analysis, N.A.M.R.; investigation, N.A.M.R., C.A.A. and K.R.M.; resources, N.A.M.R.; writing—original draft preparation, N.A.M.R.; writing—review and editing, N.A.M.R.; visualization, N.A.M.R.; supervision, C.A.A. and K.R.M. All authors have read and agreed to the published version of the manuscript.

Funding: This research received no external funding.

Informed Consent Statement: Not applicable.

Data Availability Statement: Not applicable.

Acknowledgments: This research data are part of the author's research data during the Doctor of Philosophy degree supervised by Che Aziz Bin Ali and Kamal Roslan Bin Mohamed who has retired from academia. The author would like to thank the two supervisors for their guidance during their service in the academic field.

Conflicts of Interest: The authors declare that there are no known conflicts of interest associated with this publication and there has been no significant financial support for this work that could have influenced its outcome.

References

1. Cook, H.E.; Mullins, H.T. Basin margin environments. In *Carbonate Depositional Environments: American Association of Petroleum Geologist Memoir*; Scholle, P.A., Bebout, D.G., Moore, C.H., Eds.; American Association of Petroleum Geologist: Tulsa, OK, USA, 1983; Volume 33, pp. 539–618.
2. Dasgupta, P. Sediment gravity flow—the conceptual problems. *Earth Sci. Rev.* **2003**, *62*, 265–281. [[CrossRef](#)]
3. Yang, T.; Cao, Y.; Li, Y.; Zhang, S. Status and trends in research on deep-water gravity flow deposits. *Acta Geol. Sin.* **2015**, *89*, 610–631.

4. Walker, R.G. Deep-water sandstone facies and ancient submarine fans: Models for exploration for stratigraphic traps. *AAPG Bull.* **1978**, *62*, 932–966.
5. Lowe, D.R. Sediment gravity flows: II. Depositional models with special reference to the deposits of high-density turbidity currents. *J. Sedimentol. Soc. Econ. Paleontol. Mineral.* **1982**, *52*, 279–297.
6. Middleton, G.V.; Hampton, M.A. Sediment gravity flows: Mechanics of flow and deposition. In *Turbidites and Deep-Water Sedimentation*; Society of Economy Paleontologist Mineralogist; Pacific Section SEPM: Los Angeles, CA, USA, 1973; pp. 1–38.
7. Sanders, J.E. Primary sedimentary structures formed by turbidity currents and related re-sedimentation mechanism. In *Primary Sedimentary Structures and Their Hydrodynamic Interpretation: SEPM*; Middleton, G.V., Ed.; Special Publication: Los Angeles, CA, USA, 1965; Volume 12, pp. 192–219.
8. Shanmugam, G.; Lehtonen, L.R.; Straume, T.; Syversten, S.E.; Hodgkinson, R.J.; Skibeli, M. Slump and debris flow dominated upper slope facies in the Cretaceous of the Norwegian and Northern North Seas (61–67° N): Implication for sand distribution. *AAPG Bull.* **1994**, *78*, 910–937.
9. Shanmugam, G.; Miola, R.J. Reinterpretation of depositional processes in a classic flysch sequence (Pennsylvanian Jackfork Group) Ouachita Mountains, Arkansas and Oklahoma. *Am. Assoc. Pet. Geol. Bull.* **1995**, *79*, 672–695.
10. Keunen, P.H.; Migliorini, C.I. Turbidity currents as a cause of graded bedding. *J. Geol.* **1950**, *58*, 91–127. [[CrossRef](#)]
11. Shan, Z.; Wu, H.; Ni, W.; Sun, M.; Wang, K.; Zhao, L.; Lou, Y.; Liu, A.; Xie, W.; Zheng, X. Recent technological and methodological advances for the investigation of submarine landslides. *J. Mar. Sci. Eng.* **2022**, *10*, 1728. [[CrossRef](#)]
12. Mutti, E. Turbidite systems and their relations to depositional sequences. In *Provenance of Arenites*; NATO-ASI Series; Zuffa, G.G., Ed.; Springer: Houston, TX, USA, 1985; pp. 65–93.
13. Richards, M.; Bowman, M.; Reading, H. Submarine-fan systems I: Characterization and stratigraphic prediction. *Mar. Pet. Geol.* **1998**, *15*, 689–717. [[CrossRef](#)]
14. Piper, D.J.W.; Normark, W.R. Sandy fans: From Amazon to Hueneme and beyond. *Am. Assoc. Pet. Geol. Bull.* **2001**, *85*, 1407–1438.
15. Yang, Y.; Peng, J.; Chen, Z.; Zhou, X.; Zeng, Y.; Wang, Y.; Wang, X. Depositional models of deep-water gravity-flow in lacustrine basin and its petroleum geological significance—A case study of Chang 6 Oil Group in Heshui Area, Ordos Basin, China. *Front. Earth Sci.* **2022**, *9*, 786403. [[CrossRef](#)]
16. Shanmugam, G. 50 years of the turbidite paradigm (1950s–1990s): Deep-water processes and facies models: A critical perspective. *Mar. Pet. Geol.* **2000**, *17*, 285–342. [[CrossRef](#)]
17. Shanmugam, G. New perspectives on deep-water sandstones: Implications. *Pet. Explor. Dev.* **2013**, *40*, 294–301. [[CrossRef](#)]
18. Madon, M. Submarine mass-transport deposits in the Semantan Formation (Middle—Upper Triassic), central Peninsular Malaysia. *Bull. Geol. Soc. Malays.* **2010**, *56*, 15–26. [[CrossRef](#)]
19. Akhmal, S.; Umar, H.; Rahim, A.S.; Hariri, M.A.; Radzuan, J. Deep crustal profile across NW Sabah Basin: Integrated potential field data and seismic reflection. *ARNP J. Eng. Appl. Sci.* **2016**, *11*, 1401–1411.
20. Azfar, M.; Hadi, A.A.R.; Suhaili, M.I. Sedimentary facies of the West Crocker Formation north Kota Kinabalu-Tuaran area, Sabah, Malaysia. *J. Phys. Conf. Ser.* **2015**, *10*, 142–149.
21. Ingram, G.M.; Chisholm, T.J.; Grant, C.J.; Hedlund, C.A.; Stuart-Smith, P.; Teasdale, J. Deepwater North West Borneo: Hydrocarbon accumulation in an active fold and thrust belt. *Mar. Pet. Geol.* **2004**, *21*, 879–887. [[CrossRef](#)]
22. Jackson, C.A.-L.; Zakaria, A.A.; Johnson, H.D.; Tongkul, F.; Cravello, P.D. Sedimentology, stratigraphy occurrence and origin of linked debrites in the West Crocker Formation (Oligo-Miocene), Sabah, NW Borneo. *Mar. Pet. Geol.* **2009**, *26*, 1957–1973. [[CrossRef](#)]
23. Lambiase, J.J.; Cullen, A.B. Sediment supply systems of the Champion “Delta” of NW Borneo: Implication for deep water reservoir sandstones. *J. Asian Earth Sci.* **2013**, *76*, 356–371. [[CrossRef](#)]
24. Morley, C. Geometry of an oblique thrust fault zone in a deepwater fold belt from 3D seismic data. *J. Struct. Geol.* **2009**, *31*, 1540–1555. [[CrossRef](#)]
25. Tan, D.N.K.; Lamy, J.M. Tectonic evolution of the NW Sabah continental margin since the Late Eocene. *Geol. Soc. Malays. Bull.* **1990**, *27*, 241–260. [[CrossRef](#)]
26. Tongkul, F. The Sedimentology and Structure of the Crocker Formation in the Kota Kinabalu Area, Sabah. Ph.D. Thesis, University of London, London, UK, 1987.
27. Tongkul, F. Mass transport deposit (MTD) in the Paleogene submarine fan of the Crocker Formation in Sabah, Malaysia. In *Proceedings of the Geoscience Technology Workshop, Asia Pacific Region, Kota Kinabalu, Sabah, Malaysia, 26–27 May 2015*; AAPG: Tulsa, OK, USA, 2015.
28. William, A.G.; Lambiase, J.J.; Back, S.; Jamiran, M.K. Sedimentology of the Jalan Salaiman and Bukit Melinsung outcrops, western Sabah: Is the West Crocker Formation an analogue for Neogene turbidites offshore? *Bull. Geol. Soc. Malays.* **2003**, *47*, 63–75. [[CrossRef](#)]
29. Zakaria, A.A.; Johnson, H.D.; Jackson, C.A.-L.; Tongkul, F. Sedimentary facies analysis and depositional model of the Paleogene West Crocker submarine fan system, NW Borneo. *J. Asian Earth Sci.* **2013**, *76*, 283–300. [[CrossRef](#)]
30. Jamil, M.; Siddiqui, N.A.; Rahman, A.H.A.; Ibrahim, N.A.; Ismail, M.S.; Ahmed, N.; Usman, M.; Gul, Z.; Imran, Q.S. Facies heterogeneity and lobe facies multiscale analysis of deep-marine sand-shale complexity in the West Crocker Formation of Sabah Basin, NW Borneo. *Appl. Sci.* **2021**, *11*, 5531. [[CrossRef](#)]

31. Hall, R. Cenozoic geological and plate tectonic evolution of SE Asia and the SW Pacific: Computer-based reconstructions, model and animations. *J. Asian Earth Sci.* **2002**, *20*, 353–434. [[CrossRef](#)]
32. Hutchison, C.S. Marginal basin evolution: The southern South China Sea. *Mar. Pet. Geol.* **2004**, *21*, 1129–1148. [[CrossRef](#)]
33. Hutchison, C.S.; Hall, R.; Blundell, D.J. The “Rajang Accretionary Prism” and “Lupar Line” problem of Borneo. In *Tectonic Evolution of SE Asia*; Geological Society London Special Publication: London, UK, 1996; Volume 106, pp. 247–261.
34. Liechti, P.; Roe, F.W.; Haile, N.S. The geology of Sarawak, Brunei and the western part of Borneo. *Bulletin of British Borneo. Geol. Surv.* **1960**, *3*, 360.
35. Wilson, M.E.J.; Moss, S.J. Cenozoic paleogeographic evolution of Sulawesi and Borneo. *Palaeogeogr. Palaeoclim. Palaeoecol.* **1999**, *145*, 303–337. [[CrossRef](#)]
36. Collenete, P. The geology and mineral resources of the Jesselton-Kinabalu area, north Borneo. *Br. Borneo Geol. Surv. Dept. Mem.* **1958**, *6*, 194.
37. Stauffer, P.H. Studies in the Crocker Formation, Sabah. *Malays. Geol. Surv. Bull.* **2008**, *8*, 1–13.
38. Tjia, H.D. Sense of tectonic transport in intensely deformed Trusmadi Crocker sediments, Ranau—Tenom area, Sabah. *Sains Malays.* **1974**, *3*, 129–166.
39. Tongkul, F. Regional geological correlation of Paleogene sedimentary rocks between Sabah and Sarawak, Malaysia. *GEOSEA '98 Proc. Geol. Soc. Malays. Bull.* **1999**, *45*, 31–39. [[CrossRef](#)]
40. Wilford, G.E. *Geological Map of Sabah, Scale 1:500,000*; Geological Survey of Borneo Region: Borneo Region, Malaysia, 1967.
41. Hall, R. Reconstructing Cenozoic SE Asia. In *Tectonic Evolution of SE Asia*; Geological Society London Special Publication: London, UK, 1996; Volume 106, pp. 153–184.
42. Honza, E.; John, J.; Banda, R.M. An imbrication model for the Rajang Accretionary Complex in Sarawak, Borneo. *J. Asian Earth Sci.* **2000**, *18*, 751–759. [[CrossRef](#)]
43. Baas, J.H.; Kesteren, W.V.; Postma, G. Deposits of depletive high-density turbidity currents: A flume analogue of bed geometry, structure and texture. *Sedimentology* **2004**, *51*, 1053–1088. [[CrossRef](#)]
44. Tongkul, F.; Benedick, H.; Chang, F.K. Geology of slope in the Crocker Range, Sabah, Malaysia. *J. Nepal Geol. Soc.* **2006**, *34*, 73–80. [[CrossRef](#)]
45. Tracy, G.L.; Sanudin, T.; Junaidi, A. The stratigraphy of southwest Sabah. *Bull. Geol. Soc. Malays.* **2018**, *66*, 65–74.
46. Basilici, G.; Vidal, A.C. Alternating coarse-and fine grained sedimentation in Precambrian deep-water ramp (Apiuna Formation, SE of Brazil): Tectonic and climate control or sea level variations? *Precambrian Res.* **2018**, *311*, 211–227. [[CrossRef](#)]
47. Leeder, M. *Sedimentology and Sedimentary Basins*. In *From Turbulence to Tectonics*; Blackwell Science: Oxford, UK, 1999; pp. 1–592.
48. Prothero, D.R.; Schwab, F.L. *Sedimentary Geology: An Introduction to Sedimentary Rocks and Stratigraphy*, 2nd ed.; W. H. Freeman: London, UK, 2004; pp. 1–557.
49. Boggs, S.J. *Principles of Sedimentology and Stratigraphy*, 3rd ed.; Pearson College Div., University of Oregon: Eugene, OR, USA, 2001; pp. 1–726.
50. Rohais, S.; Bailleul, J.; Brocheray, S.; Schmitz, J.; Paron, P.; Kezirian, F.; Barrier, P. Depositional model for turbidite lobes in complex slope settings along transform margins: The Motta San Giovanni Formation (Miocene—Calabria, Italy). *Front. Earth Sci.* **2021**, *9*, 766946. [[CrossRef](#)]
51. Bowen, A.J.; Normark, W.R.; Piper, A.J.W. Modelling of turbidity currents on navy Submarine Fan, California Continental Borderland. *Sedimentology* **1984**, *31*, 169–185. [[CrossRef](#)]
52. Browne, G.H.; King, P.R.; Higgs, K.E.; Slatt, R.M. Grain-size characteristics for distinguishing basin floor fan and slope fan depositional settings: Outcrop and subsurface examples from the late Miocene Mount Messenger Formation, New Zealand. *N. Z. J. Geol. Geophys.* **2005**, *48*, 213–227. [[CrossRef](#)]
53. Azpiroz-Zabala, M.; Cartigny, M.J.B.; Talling, P.J.; Parsons, D.R.; Sumner, E.J.; Clare, M.A.; Simmons, S.M.; Cooper, C.; Pope, E.L. Newly recognized turbidity current structure can explain prolonged flushing of submarine canyons. *Sci. Adv.* **2017**, *3*, e1700200. [[CrossRef](#)] [[PubMed](#)]
54. Bell, D.; Kane, I.A.; Ponten, A.S.; Flint, S.S.; Hodgson, D.M.; Barret, B.J. Spatial variability in depositional reservoir quality of deep-water channel-fill and lobe deposits. *Mar. Pet. Geol.* **2018**, *98*, 97–115. [[CrossRef](#)]
55. Garcia, M.; Ercilla, G.; Alonso, B.; Estrada, F.; Jané, G.; Mena, A.; Álvés, T.; Juan, C. Deep-water turbidite systems: A review of their elements, sedimentary processes and depositional models. Their characteristics on the Iberian margins. *Bol. Geológico Y Min.* **2015**, *126*, 189–218.
56. Lambiase, J.J.; Tan, Y.T.; William, A.G.; Bidgood, M.-D.; Brenac, P.; Cullen, A.B. The West Crocker Formation of northwest Borneo: A Paleogene accretionary prism. *Geol. Soc. Am. Spec. Pap.* **2008**, *436*, 171–184.
57. Van Hattum, M.W.A.; Hall, R.; Pickard, A.L.; Nichols, G.J. Southeast Asian sediments not from Asia: Provenance and geochronology of north Borneo sandstones. *Geol. Soc. Am.* **2006**, *34*, 589–592. [[CrossRef](#)]
58. Van Hattum, M.W.A.; Hall, R.; Pickard, A.L.; Nichols, G.J. Provenance and geochronology of Cenozoic sandstones of northern Borneo. *J. Asian Earth Sci.* **2013**, *76*, 266–282. [[CrossRef](#)]
59. Stow, D.; Smillie, Z. Distinguishing between Deep-Water Sediment Facies: Turbidites, Contourites and Hemipelagites. *Geosciences* **2020**, *10*, 68. [[CrossRef](#)]